^{1}H and ^{13}C NMR Investigation of the Influence of Nonligated Residue Contacts on the Heme Electronic Structure in Cyanometmyoglobin Complexes Reconstituted with Centro- and Pseudocentrosymmetric Hemins

Bing Hu, Jón. B. Hauksson, Anh-Tuyet T. Tran, Urzula Kolczak, Ravindra K. Pandey, Irene N. Rezzano, Kevin M. Smith, and Gerd N. La Mar*

Contribution from the Department of Chemistry, University of California, Davis, California 95616

Received May 11, 2001. Revised Manuscript Received July 19, 2001

Abstract: The ^{1}H and ^{13}C chemical shifts for the heme methyls of low-spin, ferric sperm whale cyanometmyoglobin reconstituted with a variety of centrosymmetric and pseudocentrosymmetric hemins have been recorded and analyzed to shed light on the nature of heme−protein contacts, other than that of the axial His, that modulate the rhombic perturbation to the heme's in-plane electronic asymmetry. The very similar ^{1}H dipolar shifts for heme pocket residues in all complexes yield essentially the same magnetic axes as in wild type, and the resultant dipolar shifts allow the direct determination of the heme methyl proton and ^{13}C contact shifts in all complexes. It is demonstrated that, even when the magnetic axes and anisotropies are known, the intrinsic uncertainties in the orientational parameters lead to a sufficiently large uncertainty in dipolar shift that the methyl proton contact shifts are inherently significantly less reliable indicators of the unpaired electron spin distribution than the methyl ^{13}C contact shifts. The pattern of the noninversion symmetry in ^{13}C contact shifts in the centro- or pseudocentrosymmetric hemes is shown to correlate with the positions of aromatic rings of Phe43(CD1) and His97(FG3) parallel to, and in contact with, the heme. These results indicate that such $\pi-\pi$ interactions significantly perturb the in-plane asymmetry of the heme π spin distribution and cannot be ignored in a quantitative interpretation of the heme methyl ^{13}C contact shifts in terms of the axial His orientation in *b*-type hemoproteins.

Introduction

Proton NMR spectroscopy of paramagnetic hemoproteins provides, through their hyperfine shifts, δ_{hf},[1] a wealth of functionally relevant information on the active site molecular and electronic structure that is not readily accessible in a diamagnetic derivative.[2−4] This informative δ_{hf}, however, is always accompanied by increased relaxation which invariably complicates, and sometimes obviates, the utility of the conventional 1D/2D NMR experiments needed to make assignments and define molecular structure. Nevertheless, reasonably effective NMR studies can be carried out on all paramagnetic forms,[5,6] with the degree of structural definition determined by the nature of the iron oxidation/ligation/spin state.[4] In this respect, low-spin, His-ligated hemoproteins provide the most informative ^{1}H NMR spectra, because there exist relatively well-developed interpretative bases of δ_{hf}.[2−4] Moreover, the paramagnetic relaxation is sufficiently weak so as to only minimally interfere with essentially complete assignments and, hence, allows either local heme pocket[4] or global[7,8] molecular structure determination similar to that usually carried out on diamagnetic derivatives. While there is a loss of structural information because of the diminution of NOEs near the heme, paramagnetic influences, such as dipolar shifts for nonligated residues[7−10] or the contact shift pattern for the heme,[7,8,11,12] extracted from δ_{hf} can serve as alternative constraints to compensate for lost NOEs.

The net hyperfine shift can be derived from the observed shift, δ_{obs}, if the shift of a diamagnetic analogue, δ_{dia}, is available and is composed of contact, δ_{con}, and dipolar, δ_{dip}, contributions:[2,4−6,13]

$$\delta_{hf} = \delta_{obs} - \delta_{dia} = \delta_{con} + \delta_{dip} \quad (1)$$

The contact shift, relevant only for the heme, axial His, and any sixth ligand to the iron, reflects the delocalized π spin

* Address correspondence to Dr. Gerd N. La Mar, Department of Chemistry, University of California, Davis, CA 95616. Phone: (530) 752-0958. Fax: (530) 752-8995. E-mail: lamar@indigo.ucdavis.edu.

(1) Abbreviations used: Mb, myoglobin; metMbCN, cyanide ligated ferric myoglobin; con, contact; dip, dipolar; hf, hyperfine; dia, diamagnetic; TOCSY, 2D total ^{1}H−^{1}H correlation spectroscopy; NOESY, 2D ^{1}H−^{1}H nuclear Overhauser spectroscopy; DSS, 2,2-dimethyl-2-silapentane-5-sulfonate; HMQC, heteronuclear multi-quantum coherence.

(2) Bertini, I.; Turano, P.; Villa, A. J. *Chem. Rev.* **1993**, *93*, 2833−2932.
(3) Yamamoto, Y. *Annu. Rep. NMR Spectrosc.* **1998**, *36*, 1−77.
(4) La Mar, G. N.; Satterlee, J. D.; de Ropp, J. S. In *The Porphyrin Handbook*; Kadish, K., Smith, K., Guilard, R., Eds.; Academic Press: Boston, 1999; Vol. 5.
(5) La Mar, G. N.; de Ropp, J. S. *Biol. Magn. Reson.* **1993**, *18*.
(6) Bertini, I.; Luchinat, C. *Coord. Chem. Rev.* **1996**, *150*, 1−296.
(7) Turner, D. L.; Brennan, L.; Chamberlin, S. G.; Louro, R. O.; Xavier, A. V. *Eur. Biophys. J.* **1998**, *27*, 367−375.
(8) Banci, L.; Bertini, I.; Luchinat, C.; Turano, P. In *The Porphyrin Handbook*; Kadish, K. M., Smith, K. M., Guilard, R., Eds.; Academic Press: Boston, 1999; Vol. 5, pp 323−350.
(9) Clayden, N. J.; Moore, G. R.; Williams, G. *Met. Ions Biol. Syst.* **1987**, *21*, 187−227.
(10) Bertini, I.; Luchinat, C.; Rosato, A. *Prog. Biophys. Mol. Biol.* **1996**, *66*, 43−80.
(11) Bertini, I.; Luchinat, C.; Parigi, G.; Walker, F. A. *J. Biol. Inorg. Chem.* **1999**, *4*, 515−519.
(12) Turner, D. L. *J. Biol. Inorg. Chem.* **2000**, *5*, 328−332.

10.1021/ja011175r CCC: $20.00
Published on Web 09/22/2001

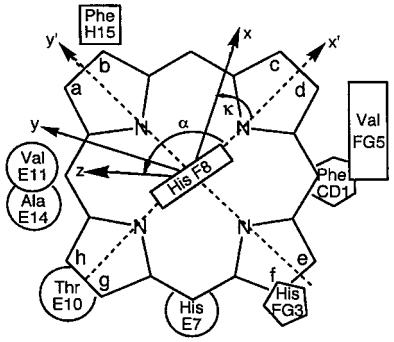

Figure 1. Schematic structure of the heme cavity in sperm whale Mb as viewed from the proximal side. Two aromatic rings parallel to, and in contact with, the heme are the proximal His97(FG3) imidazole ring and the distal Phe43(CD1) benzene ring. Other proximal and distal residues of interest are shown in rectangles and circles, respectively. The heme positions for an arbitrary hemin are labeled a−h and correspond, respectively, to positions 1−8 occupied by native protohemin (**1**). The orientation of the magnetic axes, *x*, *y*, *z*, relative to the iron-centered, reference coordinate system, *x*′, *y*′, *z*′, is defined by the tilt, β, of the major magnetic axes, *z*, from the heme normal, in direction α, as defined by the projection of *z* on the heme plane; the *x*′ axis, with the projection of the rhombic axes on the heme plane, is given by $\kappa \sim \alpha + \gamma$.

density, ρ_π, which, for a core methyl group nucleus *i* is given by[6]

$$\delta^{i}_{\mathrm{con}} = \frac{Q(i)\rho_\pi}{\gamma_i \hbar B_o}\langle S_z\rangle \qquad (2)$$

where *Q* is a constant for a methyl proton, $Q(\mathrm{C^1H_3}) = \sim 70$ MHz, and a methyl carbon, $Q(^{13}\mathrm{CH_3}) = \sim -40$ MHz, B_o is the magnetic field strength, γ_i is the magnetogyric ratio for nucleus *i*, and $\langle S_z\rangle$ is the electron spin-magnetization. The dipolar shift, which is experienced by all nuclei, is given by[10,13,14]

$$\delta_{\mathrm{dip}} = \delta^{\mathrm{M}}{}_{\mathrm{dip}} + \delta^{\mathrm{L}}{}_{\mathrm{dip}} \qquad (3)$$

where the shift due to the dominant, metal(iron)-centered dipolar interaction, $\delta^{\mathrm{M}}{}_{\mathrm{dip}}$, is given by

$$\delta^{\mathrm{M}}{}_{\mathrm{dip}} = (12\pi \mathrm{N_A})^{-1}[2\Delta\chi_{\mathrm{ax}}(3\cos^2\theta'_i - 1)R^{-3}{}_i + 3\Delta\chi_{\mathrm{rh}}(\sin^2\theta'_i \cos 2\Omega)R^{-3}]\Gamma(\alpha,\beta,\gamma) \qquad (4)$$

Here, *R*, θ', and Ω' are the coordinates of a nucleus in some arbitrary, iron-centered coordinate system, *x*′, *y*′, *z*′ (or *R*, θ', Ω'), as shown in Figure 1, *x*, *y*, and *z* are the magnetic coordinates in which the paramagnetic susceptibility tensor, χ, is diagonal, and $\Delta\chi_{\mathrm{ax}}$ and $\Delta\chi_{\mathrm{rh}}$ are the axial and rhombic anisotropies. The Euler angles, α, β, γ, rotate the reference into the magnetic coordinate system.[4,15,16] The term $\delta^{\mathrm{L}}{}_{\mathrm{dip}}$ in eq 3 reflects ligand-centered dipolar shifts,[13,14] is nonzero only for heteronuclei (i.e., ^{13}C), but is known to be small in low-spin ferric hemoproteins.[17,18]

A 4-fold symmetric low-spin ferric heme possesses a single unpaired spin shared by the degenerate d_{xz} and d_{yz} orbitals, which results in equal π spin delocalization and hence equal $\delta_{\mathrm{con}}(\mathrm{CH_3})$, for the four pyrrole rings.[4,11,12,19−23] The introduction of such a 4-fold symmetric hemin into a protein matrix raises the d_{xz} and d_{yz} orbital degeneracy,[19] forces the lone spin to largely populate one of the two linear combinations of the d_{xz} and d_{yz} orbitals, and results in a significant increase in the asymmetry for $\delta_{\mathrm{con}}(\mathrm{CH_3})$ or ρ_π for the four pyrroles.[2,4,20,23] The orbital ground state, and hence methyl contact shift pattern, is determined, in large part, by the orientation of the axial His imidazole plane(s) relative to the heme.[2,4,11,12,17,21,24−27] If the major magnetic axis is normal to the heme such as in cytochrome *c*,[21,26] the His orientation can be related to the pattern of the combination of δ_{dip} and δ_{con}.[11,12,27] For other cases where the major magnetic axis is tilted significantly from the heme normal, such as in globins[4,16,28−32] and peroxidases,[33,34] the magnetic axes must be determined first. This is particularly true for heme methyl protons where δ_{con} and δ_{dip} can have comparable magnitudes. However, because a given ρ_π yields[6,21,26,35] a much larger $\delta_{\mathrm{con}}(^{13}\mathrm{CH_3})$ than $\delta_{\mathrm{con}}(\mathrm{C^1H_3})$, $\delta_{\mathrm{hf}}(^{13}\mathrm{CH_3})$ can serve as an approximation[18,21] of $\delta_{\mathrm{con}}(^{13}\mathrm{CH_3})$.

There are, however, numerous interactions other than the axial His orientation which are capable of modulating the heme in-plane asymmetry, such as the nature of heme peripheral substituents[32,35,36] (vinyls in native hemin, **1**; M = methyl, P = propionate, V = vinyl), van der Waals interactions between the porphyrin and residues in contact with it, and distortion(s) of the heme planarity by nonspecific protein interactions, among others. In fact, asymmetric peripheral substitutions of all natural hemins actually introduce a variable asymmetry in the ρ_π or $\delta_{\mathrm{con}}(\mathrm{CH_3})$ distribution even outside the protein matrix,[17,20,23,32,35−37] so that the natural hemins possess, at best, pseudo-4-fold symmetry. It is known that different alkyl substituents (methyl, ethyl, propionyl) inconsequentially perturb the 4-fold symmetry

(13) Kurland, R. J.; McGarvey, B. R. *J. Magn. Reson.* **1970**, *2*, 286−301.
(14) Mispelter, J.; Momenteau, M.; Lhoste, J.-M. *Biol. Magn. Reson.* **1993**, *12*, 229−355.
(15) Williams, G.; Clayden, N. J.; Moore, G. R.; Williams, R. J. P. *J. Mol. Biol.* **1985**, *183*, 447−460.
(16) Emerson, S. D.; La Mar, G. N. *Biochemistry* **1990**, *29*, 1556−1566.
(17) Banci, L.; Bertini, I.; Pierattelli, R.; Vila, A. J. *Inorg. Chem.* **1994**, *33*, 4338−4343.
(18) Brennan, L.; Turner, D. L. *Biochim. Biophys. Acta* **1997**, *1342*, 1−12.
(19) Shulman, R. G.; Glarum, S. H.; Karplus, M. *J. Mol. Biol.* **1971**, *57*, 93−115.
(20) Walker, F. A.; Simonis, U. *Biol. Magn. Reson.* **1993**, *12*.
(21) Turner, D. L. *Eur. J. Biochem.* **1995**, *227*, 829−837.
(22) Turner, D. L.; Salgueiro, C. A.; Catarino, T.; Legall, J.; Xavier, A. V. *Eur. J. Biochem.* **1995**, *241*, 723−731.
(23) Walker, F. A. In *The Porphyrin Handbook*; Kadish, K. M., Guillard, R., Smith, K. M., Eds.; Academic Press: Boston, 1999; Vol. 5, pp 81−183.
(24) Traylor, T. G.; Berzinis, A. P. *J. Am. Chem. Soc.* **1980**, *102*, 2844−2846.
(25) Qin, J.; La Mar, G. N.; Ascoli, F.; Brunori, M. *J. Mol. Biol.* **1993**, *231*, 1009−1023.
(26) Turner, D. L.; Salgueiro, C. A.; Schenkels, P.; LeGall, J.; Xavier, A. V. *Biochim. Biophys. Acta* **1995**, *1246*, 24−28.
(27) Shokhirev, N. V.; Walker, F. A. *J. Biol. Inorg. Chem.* **1998**, *3*, 581−594.
(28) Rajarathnam, K.; Qin, J.; La Mar, G. N.; Chiu, M. L.; Sligar, S. G. *Biochemistry* **1993**, *32*, 5670−5680.
(29) Banci, L.; Pierattelli, R.; Turner, D. L. *Eur. J. Biochem.* **1995**, *232*, 522−527.
(30) Wu, Y.; Chien, E. Y. T.; Sligar, S. G.; La Mar, G. N. *Biochemistry* **1998**, *37*, 6979−6990.
(31) Nguyen, B. D.; Xia, Z.; Yeh, D. C.; Vyas, K.; Deaguero, H.; La Mar, G. *J. Am. Chem. Soc.* **1999**, *121*, 208−217.
(32) Kolczak, U.; Hauksson, J. B.; Davis, N. L.; Pande, U.; de Ropp, J. S.; Langry, K. C.; Smith, K. M.; La Mar, G. N. *J. Am. Chem. Soc.* **1999**, *121*, 835−843.
(33) La Mar, G. N.; Chen, Z.; Vyas, K.; McPherson, A. D. *J. Am. Chem. Soc.* **1995**, *117*, 411−419.
(34) Banci, L.; Bertini, I.; Pierattelli, R.; Tien, M.; Vila, A. J. *J. Am. Chem. Soc.* **1995**, *117*, 8659−8667.
(35) Wüthrich, K.; Baumann, R. *Helv. Chim. Acta* **1974**, *57*, 336−350.
(36) La Mar, G. N.; Viscio, D. B.; Smith, K. M.; Caughey, W. S.; Smith, M. L. *J. Am. Chem. Soc.* **1978**, *100*, 8085−8092.
(37) Yamamoto, Y.; Nanai, N.; Inoue, Y.; Chujo, R. *Biochem. Biophys. Res. Commun.* **1988**, *151*, 262−269.

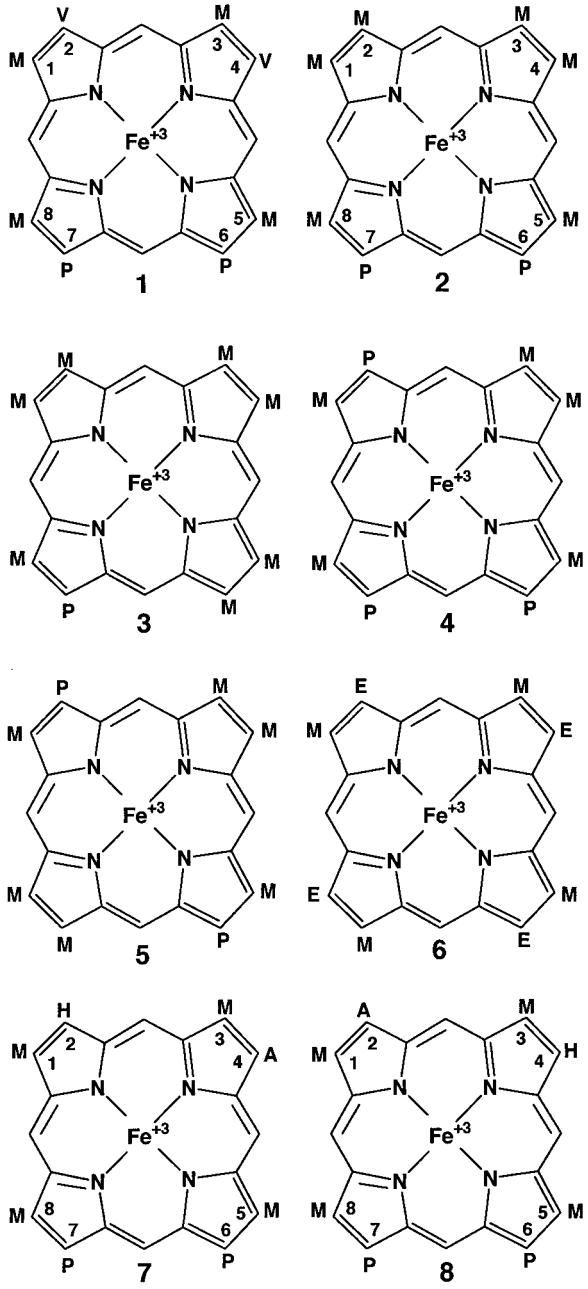

in low-spin models, as evidenced by the very similar $\delta_{hf}(CH_3)$ for the four methyls of the biscyano complexes of mesohemin[36] (which possesses methyl, propionyl, and ethyl substituents). In the case of the *c*-type cytochromes, all eight substituents are alkyl groups such that substituent effects are likely very small.[38] It is obvious, however, that this is not the case for *b*-type hemoproteins that contain protohemin,[36] (**1**), such as globins, peroxidases, and *b*-type cytochromes. Rhombic influences of heme peripheral substituents comparable in magnitude to those of the axial His orientation have been demonstrated[32] for some acetyl- (i.e., hemins **7** and **8**) and formyl-substituted hemins reconstituted into Mb.

Direct evidence for significant contributions from influences to the rhombic asymmetry of the heme other than the axial His is the lack of inversion symmetry through the iron for $\delta_{hf}(CH_3)$, although both δ_{dip} and δ_{con} are expected to reflect such symmetry. This deviation from inversion symmetry may be small in cytochromes *c* but is large in globins.[4,39−41] In this report, we are interested in elucidating the origin of heme *in-plane asymmetry in globins induced by protein interactions other than those from the axial His*. To this end, we have reconstituted a variety of approximately, as well as two truly, centrosymmetric hemins into low-spin, ferric cyanomet sperm whale Mb, and analyzed the δ_{hf} in terms of δ_{con} for both ^{1}H and ^{13}C for the heme methyls. The previously determined magnetic axes and anisotropies of WT (wild type) metMbCN[31] are shown to be minimally perturbed by the chemical modifications of the heme,[32] thereby allowing separation of δ_{con} and δ_{dip} for the heme methyls. The hemins selected are pseudo-4-fold symmetric hemins possessing solely methyl and propionate pyrrole substituents, **2**−**4**, and exhibiting $\delta_{hf}(CH_3)$ as biscyano complexes that differ by ≤ 5% among the methyls, and truly centrosymmetric hemins **5** and **6** (etiohemin I). Also included in this study are two hemins, **7** (2-acetyl-deuteriohemin) and **8** (4-acetyl-deuteriohemin) (M = methyl, P = propionate, H = hydrogen, A = acetyl), which possess strong electronic asymmetry due to the electron withdrawing acetyl substituent.[32] The heme and numerous heme pocket residue proton signals for metMbCN reconstituted with hemins **1**−**8** have been assigned, and the orientations of each of the hemins in the heme pocket have been reported.[32,39−43]

Experimental Section

Reconstitution of Mb. The sperm whale metMb(***q***)CN samples of hemin ***q***, with ***q*** = **1**−**8**, are the same samples described in detail previously.[32,39−41,43] Each sample consisted of ∼50 mM phosphate and ∼100 mM NaCl in ^2H_2O at pH 7.5−8.2, in which range the chemical shifts are essentially independent of pH.

NMR Spectra. All spectra were recorded on a Bruker AVANCE 500 spectrometer operating at 500 MHz for ^{1}H and 125 MHz for ^{13}C. ^{1}H steady-state NOEs were recorded as described in detail previously.[28,30] Nonselective T_1's were estimated from the initial recovery of the magnetization in an inversion−recovery experiment. All chemical shifts are referenced to 2,2- dimethyl-2-silapentane-5-sulfonate, DSS, via the residual solvent signal. ^{1}H NMR TOCSY[44] (25 ms mixing time) and NOESY[45] (40 ms mixing time) spectra were recorded over 25−30 kHz spectral windows using 512 t1 blocks of 96 scans each and 2048 t2 points with repetition rates of 1−3 s^{-1}. The 2D data were apodized by a 20−30° sine-bell-squared function and zero-filled to 2048 × 2048 points prior to Fourier transformation on a Silicon Graphics Indigo Workstation using the XWIN NMR programs. ^{1}H-detected {^{1}H−^{13}C}-HMQC spectra[46] at natural abundance were recorded over 36 kHz bandwidth centered on H_2O and 25 kHz spectral width centered on dioxane and consisted of 512 t1 blocks of 332 scans and 1024 t2 points with transfer time of 2.7 ms. The ^{13}C chemical shifts were calibrated with dioxane at 66.6 ppm relative to DSS.

The heme $\delta_{dia}(C^1H_3)$ for hemin **1** were taken from Mb(**1**)CO.[47] Comparison of the $\delta_{dia}(C^1H_3)$ in a diamagnetic hemin **1** iron(II) complex[37,48] with Mb(**1**)CO reveals that protein-based ring currents

(38) Louro, R. O.; Correia, I. J.; Brennan, L.; Coutinho, I. B.; Xavier, A. V.; Turner, D. L. *J. Am. Chem. Soc.* **1998**, *120*, 13240−13247.

(39) La Mar, G. N.; Emerson, S. D.; Lecomte, J. T. J.; Pande, U.; Smith, K. M.; Craig, G. W.; Kehres, L. A. *J. Am. Chem. Soc.* **1986**, *108*, 5568−5573.

(40) Hauksson, J. B.; La Mar, G. N.; Pandey, R. K.; Rezzano, I. N.; Smith, K. M. *J. Am. Chem. Soc.* **1990**, *112*, 6198−6205.

(41) Hauksson, J. B.; La Mar, G. N.; Pandey, R. K.; Rezzano, I. N.; Smith, K. M. *J. Am. Chem. Soc.* **1990**, *112*, 8315−8323.

(42) Emerson, S. D.; La Mar, G. N. *Biochemistry* **1990**, *29*, 1545−1555.

(43) Tran, A.-T.; Kalish, H.; Balch, A. L.; La Mar, G. N. *J. Biol. Inorg. Chem.* **2000**, *5*, 624−633.

(44) Griesinger, C.; Otting, G.; Wüthrich, K.; Ernst, R. R. *J. Am. Chem. Soc.* **1988**, *110*, 7870−7872.

(45) Jeener, J.; Meier, B. H.; Bachmann, P.; Ernst, R. R. *J. Chem. Phys.* **1979**, *71*, 4546−4553.

(46) Bax, A.; Griffey, R. H.; Hawkins, B. L. *J. Magn. Reson.* **1983**, *55*, 301−315.

(47) Thériault, Y.; Pochapsky, T. C.; Dalvit, C.; Chiu, M. L.; Sligar, S. G.; Wright, P. E. *J. Biomol. NMR* **1994**, *4*, 491−504.

Table 1. Heme Methyl Proton and Carbon 13 Shifts in MetMb(***q***)CN Reconstituted with Hemins ***q*** = **1**−**8**[a]

		C^1H_3					$^{13}CH_3$					
hemin	position[a]	δ_{obs}[b]	δ_{dia}[c]	δ_{hf}[d]	δ_{dip}[e]	δ_{con}[f]	δ_{obs}[b]	δ_{dia}[c]	δ_{hf}[d]	$\delta^{Fe}{}_{dip}$[e]	δ_{con}[f]	$\delta_{con}(^{13}CH_3)/\delta_{con}(C^1H_3)$
1	a(1)	18.1	3.6 ± 0.2	14.5 ± 0.2	−3.6 ± 0.9	18.1 ± 1.1	−37.8	13.0 ± 0.5	−50.8 ± 0.5	−4.5 ± 1.2	−46.3 ± 1.7	−2.6 ± 0.2
	c(3)	5.1	3.8 ± 0.2	1.3 ± 0.2	−4.2 ± 0.8	5.5 ± 1.0	−13.4	13.0 ± 0.5	−26.4 ± 0.5	−5.3 ± 1.0	−21.1 ± 1.5	−3.8 ± 0.8
	e(5)	26.6	2.5 ± 0.2	24.1 ± 0.2	−3.4 ± 0.9	27.5 ± 1.1	−58.5	10.5 ± 0.5	−69.0 ± 0.5	−4.2 ± 1.0	−64.8 ± 1.5	−2.4 ± 0.2
	h(8)	12.8	3.6 ± 0.2	9.2 ± 0.2	−4.8 ± 1.0	14.0 ± 1.2	−32.2	11.5 ± 0.5	−43.7 ± 0.5	−6.2 ± 1.3	−37.5 ± 1.8	−2.7 ± 0.3
2	a(1)	21.5	3.7 ± 0.2	17.8 ± 0.2	−3.6 ± 0.9	21.4 ± 1.1	−47.4	11.7 ± 0.5	−59.1 ± 0.5	−4.5 ± 1.2	−54.6 ± 1.7	−2.6 ± 0.2
	b(2)	18.8	3.7 ± 0.2	15.1 ± 0.2	−3.6 ± 1.2	18.7 ± 1.4	−43.2	11.7 ± 0.5	−54.9 ± 0.5	−4.5 ± 1.6	−50.4 ± 2.1	−2.7 ± 0.3
	c(3)	6.5	3.7 ± 0.2	2.8 ± 0.2	−4.2 ± 0.8	7.0 ± 1.0	−19.0	11.7 ± 0.5	−30.7 ± 0.5	−5.4 ± 1.0	−25.3 ± 1.5	−3.6 ± 0.6
	d(4)	9.6	3.7 ± 0.2	5.9 ± 0.2	−4.1 ± 0.9	10.0 ± 1.1	−24.0	11.7 ± −0.5	−35.7 ± 0.5	−5.3 ± 1.1	−30.4 ± 1.6	−3.0 ± 0.4
	e(5)	24.5	2.5 ± 0.2	22.0 ± 0.2	−3.4 ± 0.9	25.4 ± 1.1	−55.5	10.7 ± 0.5	−66.2 ± 0.5	−4.2 ± 1.0	−62.0 ± 1.5	−2.5 ± 0.1
	h(8)	11.8	3.6 ± 0.2	8.2 ± 0.2	−4.8 ± 1.0	13.0 ± 1.2	−31.2	11.7 ± 0.5	−42.9 ± 0.5	−6.2 ± 1.3	−36.7 ± 1.8	−2.8 ± 0.3
3	a(1)	22.0	3.7 ± 0.2	18.3 ± 0.2	−3.6 ± 0.9	21.9 ± 1.1	−48.3	11.7 ± 0.5	−60.0 ± 0.5	−4.5 ± 1.2	−55.5 ± 1.7	−2.5 ± 0.2
	b(2)	19.1	3.7 ± 0.2	15.2 ± 0.2	−3.6 ± 1.2	18.8 ± 1.4	−43.7	11.7 ± 0.5	−55.4 ± 0.5	−4.5 ± 1.6	−50.9 ± 2.1	−2.7 ± 0.3
	c(3)	6.7	3.7 ± 0.2	3.0 ± 0.2	−4.2 ± 0.8	7.2 ± 1.0	−19.7	11.7 ± 0.5	−31.4 ± 0.5	−5.4 ± 1.0	−26.0 ± 1.5	−3.6 ± 0.7
	d(4)	9.0	3.7 ± 0.2	5.3 ± 0.2	−4.1 ± 0.9	9.4 ± 1.1	−23.1	11.7 ± 0.5	−34.8 ± 0.5	−5.3 ± 1.1	−29.5 ± 1.6	−3.1 ± 0.5
	e(5)	25.6	2.5 ± 0.2	23.1 ± 0.2	−3.4 ± 0.5	26.5 ± 1.1	−57.2	10.7 ± 0.5	−67.9 ± 0.5	−4.2 ± 1.0	−63.7 ± 1.5	−2.4 ± 0.2
	f(6)	22.7	2.7 ± 0.2	20.0 ± 0.2	−3.2 ± 1.2	23.2 ± 1.4	−50.3	10.9 ± 0.5	−61.2 ± 0.5	−4.1 ± 1.4	−57.1 ± 1.9	−2.5 ± 0.3
	h(8)	11.2	3.6 ± 0.2	7.6 ± 0.2	−4.8 ± 1.0	12.4 ± 1.2	−30.4	11.7 ± 0.5	−42.1 ± 0.5	−6.2 ± 1.3	−35.9 ± 1.8	−2.9 ± 0.4
4	a(1)	19.5	3.7 ± 0.2	15.8 ± 0.2	−3.6 ± 0.9	19.4 ± 1.1	−44.7	11.7 ± 0.5	−56.4 ± 0.5	−4.5 ± 1.2	−51.9 ± 1.7	−2.7 ± 0.2
	c(3)	6.8	3.7 ± 0.2	3.1 ± 0.2	−4.2 ± 0.8	7.3 ± 1.0	−18.9	11.7 ± 0.5	−30.6 ± 0.5	−5.4 ± 10	−25.2 ± 1.3	−3.4 ± 0.6
	d(4)	9.6	3.7 ± 0.2	5.9 ± 0.2	−4.1 ± 0.9	10.0 ± 1.1	−25.3	11.7 ± 0.5	−37.0 ± 0.5	−5.3 ± 1.0	−31.7 ± 1.5	−3.1 ± 0.5
	e(5)	24.1	2.5 ± 0.2	21.6 ± 0.2	−3.4 ± 0.9	25.0 ± 1.1	−54.6	10.7 ± 0.5	−65.3 ± 0.5	−4.2 ± 1.0	−61.1 ± 1.5	−2.5 ± 0.2
	h(8)	12.1	3.6 ± 0.2	8.5 ± 0.0	−4.8 ± 1.0	13.3 ± 1.2	−32.5	11.7 ± 0.5	−44.2 ± 0.5	−6.2 ± 1.3	−38.0 ± 1.8	−2.8 ± 0.3
5	a(1)	18.3	3.7 ± 0.2	14.6 ± 0.2	−3.6 ± 0.9	18.2 ± 1.1	−42.2	11.7 ± 0.5	−53.9 ± 0.5	−4.5 ± 1.2	−49.4 ± 1.7	−2.7 ± 0.2
	c(3)	8.4	3.7 ± 0.2	4.7 ± 0.2	−4.2 ± 0.8	8.9 ± 1.0	−24.5	11.7 ± 0.5	−36.2 ± 0.5	−5.4 ± 1.0	−30.8 ± 1.5	−3.4 ± 0.5
	d(4)	9.3	3.7 ± 0.2	5.6 ± 0.2	−4.1 ± 0.9	9.8 ± 1.1	−25.8	11.7 ± 0.5	−37.5 ± 0.5	−5.3 ± 1.0	−32.2 ± 1.5	−3.3 ± 0.4
	e(5)	21.7	2.5 ± 0.2	19.2 ± 0.2	−3.4 ± 0.9	22.6 ± 1.1	−49.9	10.7 ± 0.5	−60.6 ± 0.5	−4.2 ± 1.0	−56.4 ± 1.5	−2.5 ± 0.2
	g(7)	10.0	3.7 ± 0.2	6.3 ± 0.2	−4.3 ± 0.8	10.6 ± 1.0	−25.7	11.7 ± 0.5	−32.4 ± 0.5	−5.8 ± 1.0	−31.6 ± 1.5	−3.0 ± 0.4
	h(8)	12.2	3.6 ± 0.2	8.6 ± 0.2	−4.8 ± 1.0	13.4 ± 1.2	−31.6	11.7 ± 0.5	−43.3 ± 0.5	−6.2 ± 1.3	−37.1 ± 1.8	−2.8 ± 0.3
6	a(1)	20.3	3.7 ± 0.2	16.6 ± 0.2	−3.6 ± 0.9	20.2 ± 1.1	−4.51	11.7 ± 0.5	−56.8 ± 0.5	−4.5 ± 1.2	−52.3 ± 1.7	−2.6 ± 0.2
	c(3)	7.8	3.7 ± 0.2	4.1 ± 0.2	−4.2 ± 0.8	8.3 ± 1.0	−23.2	11.7 ± 0.5	−34.9 ± 0.5	−5.4 ± 1.0	−29.5 ± 1.5	−3.5 ± 0.6
	e(5)	23.7	2.5 ± 0.2	21.2 ± 0.2	−3.4 ± 0.9	24.6 ± 1.1	−53.8	10.7 ± 0.5	−64.5 ± 0.5	−4.2 ± 1.0	−60.3 ± 1.5	−2.5 ± 0.2
	g(7)	7.7	3.7 ± 0.2	4.0 ± 0.2	−4.3 ± 0.8	8.3 ± 1.0	−23.2	11.7 ± 0.5	−35.4 ± 0.5	−5.8 ± 1.0	−29.6 ± 1.5	−3.5 ± 0.6
7	a(1)	16.1	3.7 ± 0.2	12.4 ± 0.2	−3.6 ± 0.9	16.0 ± 1.1	−29.4	13.0 ± 0.5	−42.4 ± 0.5	−4.5 ± 1.2	−37.9 ± 1.7	−2.4 ± 0.5
	c(3)	3.9	3.7 ± 0.2	0.2 ± 0.2	−4.2 ± 0.8	4.4 ± 1.0	−11.6	13.0 ± 0.5	−24.6 ± 0.5	−5.4 ± 1.0	−19.2 ± 1.5	−4.3 ± 0.9
	e(5)	30.3	2.5 ± 0.2	27.8 ± 0.2	−3.4 ± 0.9	31.2 ± 1.1	−63.8	10.5 ± 0.5	−74.3 ± 0.5	−4.2 ± 1.0	−70.1 ± 1.5	−2.3 ± 0.2
	h(8)	10.4	3.6 ± 0.2	6.8 ± 0.2	−4.8 ± 1.0	11.6 ± 1.2	−28.1	11.5 ± 0.5	−39.6 ± 0.5	−6.2 ± 1.3	−33.4 ± 1.8	−2.8 ± 0.4
8	a(1)	8.5	3.7 ± 0.2	4.8 ± 0.2	−3.6 ± 0.9	8.4 ± 1.1	−19.7	13.0 ± 0.5	−32.7 ± 0.5	−4.5 ± 1.2	−28.2 ± 1.7	−3.3 ± 0.6
	c(3)	11.6	3.7 ± 0.2	7.9 ± 0.2	−4.2 ± 0.8	12.1 ± 1.0	−25.3	13.0 ± 0.5	−38.3 ± 0.5	−5.4 ± 1.0	−32.9 ± 1.5	−2.7 ± 0.3
	e(5)	20.0	2.5 ± 0.2	17.5 ± 0.2	−3.4 ± 0.9	20.9 ± 1.1	−48.8	10.5 ± 0.5	−59.3 ± 0.5	−4.2 ± 1.0	−55.1 ± 1.5	−2.6 ± 0.2
	h(8)	19.4	3.0 ± 0.2	15.8 ± 0.2	−4.8 ± 1.0	20.6 ± 1.2	−44.6	11.5 ± 0.5	−56.1 ± 0.5	−6.2 ± 1.3	−49.9 ± 1.8	−2.4 ± 0.3

[a] Positions a−h correspond to positions within the heme pocket, as shown in Figure 1 (in parentheses are the labels that correspond to positions 1−8 occupied by native hemin **1**). [b] Observed shift, in ppm referenced to DSS, in ^2H_2O at 30 °C. [c] Diamagnetic chemical shift, in ppm, referenced to DSS. [d] Hyperfine shift, in ppm, at 30 °C, obtained from eq 1. [e] Dipolar shift, in ppm at 30 °C, obtained from eq 4, using the coordinates of octamethyl heme inserted into MbCO[50] for the magnetic axes $\alpha = -10 \pm 10°$, $\beta = 14 \pm 2°$, and $\kappa = -10° \pm 15°$ and the WT $\Delta\chi_{ax} = 2.3 \times 10^{-9}$ m^3/mol and $\Delta\chi_{rh} = -0.57 \times 10^{-9}$ m^3/mol.[31] [f] Contact shift, in ppm at 30 °C, obtained from eq 1.

result in small (∼1 ppm) upfield 5-CH_3 and 6-CH shifts due to the aromatic rings of Phe CD1 and His FG3. The $\delta_{dia}(C^1H_3)$ for other hemins, and the $\delta_{dia}(^{13}CH_3)$ for all complexes, were obtained by adding the protein-based ring-current perturbation to the shifts for diamagnetic model complexes.[17,35,37,48] The range of heme methyl ^{13}C chemical shifts for a variety of hemes with only alkyl substituents is very small (0.3 ppm) such that the reported values[48] can be considered valid for all the hemes of current interest. The uncertainties in $\delta_{dia}(C^1H_3)$ and $\delta_{dia}(^{13}CH_3)$ are estimated at ±0.2 and ±0.5 ppm, respectively. The resulting δ_{dia}, listed in Table 1, lead to δ_{hf} via eq 1.

Magnetic Axes. The orientation of the magnetic axes was determined for each metMbCN complex by minimizing the global error function, F/n:[4,15,16]

$$F/n = \sum^{n} |\delta_{dip}(obs) - \delta_{dip}(calc)|^2 \qquad (5)$$

where the observed dipolar shift for nonligated residue protons,[49] δ_{dip}(obs), is given by eq 1 with $\delta_{con} = 0$; $\Delta\chi_{ax} = 2.56 \times 10^{-8}$ m^3/mol and $\Delta\chi_{rh} = -0.58 \times 10^{-8}$ m^3/mol are the axial and rhombic anisotropies that have been accurately determined for metMbCN[31] and found to be invariant over a wide range of cyanomet Mb and Hb complexes.[4,28,30] The values of δ_{dia} in eq 1 for nonligated residues were taken from MbCO.[47] The orientation of the magnetic axes is described by tilt β of the major axis from the heme normal, in a direction defined by α, the angle between the z axis projection on the heme plane and the x' axis, with the rhombic axes defined by $\kappa \sim \alpha + \gamma$, as shown in Figure 1. The resulting magnetic axes allowed the determination of $\delta^{M}{}_{dip}(C^1H_3)$ and $\delta^{M}{}_{dip}(^{13}CH_3)$ via eq 4 and, assuming $\delta^{L}{}_{dip} \sim 0$ for ^{13}C, leads to $\delta_{con}(C^1H_3)$ and $\delta_{con}(^{13}CH_3)$, via eq 1.

Results

^{1}H NMR Assignments. The 500 MHz ^{1}H NMR spectra at 25 °C of WT metMbCN and the cyanomet complex of sperm whale Mb reconstituted with synthetic hemins **2**−**8** are repro-

(48) Medforth, C. J. In *The Porphyrin Handbook*; Kadish, K., Smith, K. M., Guilard, R., Eds.; Academic Press: Boston, 1999; Vol. 5, pp 1−80.

(49) The magnetic anisotropies for WT metMbCN[31] and dipolar shifts for the same residue protons were used in each magnetic axes determination: Phe43(CD31) [C_δHs, C_ϵHs, C_ζH], Val68(E11) [C_αH, C_βH]; Ala71-(E14) [C_αH, $C_\beta H_3$], Leu89(F4) [C_αH], Ala90(F5) [C_αH, $C_\beta H_3$]; His93(F38) [NH, C_αH], His97(FG3) [C_δH], Ile99(FG5) [C_αH, C_βH, C_αHs, $C_\gamma H_3$, $C_\delta H_3$].

duced in Figure 2A−H, respectively. The complete heme pyrrole methyl proton signals in complexes of hemins **1**−**8** have been reported,[16,32,39−41,43] as well as the key residues in the complexes of hemins **2**, **6**, **7**, and **8**. To describe both the positions of a methyl on the heme and the location of that methyl in the heme pocket, two different labeling schemes are necessary. For protohemin, **1**, the hemin-based conventional Fisher notation is used that labels the pyrrole positions 1−8, with propionates at positions 6 and 7. To describe the position that a hemin methyl can adopt in the protein matrix, we label the eight possible protein-based positions by a−h, as shown in Figure 1. The correlation between 1−8 and a−h depends on the orientation of the hemin in the heme pocket. For native protohemin, **1**, as well as hemins **2**, **7**, and **8**, the protein-based positions a−h are occupied by heme-based positions 1−8, respectively. For the other hemins, there is no unique numbering system intrinsic to the hemin so that the methyls are labeled solely by the positions a−h they occupy in the protein matrix, as determined and discussed in detail previously.[40,41,43] Hence, resonances in Figure 2 are labeled M_i (methyl, H_i (single proton)), where *i* is the position on the heme periphery (M_1 for the hemin-based position or M_a for the protein-based position, methyl at position 1 or position a) or the residue (i.e., H_{CD1} is $C_\xi H$ of Phe CD1, and M_{FG5}, H_{FG5} are methyl and proton of Ile FG5). The key dipolar shifted heme pocket residues needed[16,28,30−32] to determine the magnetic axes and define heme orientation[30] are Phe43(CD1), His64(E7), Val68(E11), Ala71(E14), Leu89(F4), His93(F8), His97(FG3), and Ile99(FG5).

Earlier partial assignments[40,41] of Phe43(CD1), His93(F8), His64(E10), and Ile99(FG5) based on steady-state NOEs for hemins **3**−**5** in metMbCN are herein augmented by standard 2D analysis as reported for numerous metMbCN complexes (not shown).[16] The ^{1}H NMR chemical shift of the heme methyls at 25 °C are summarized in Table 1, and the chemical shifts for the key residues are listed in Supporting Information. The expected,[42,50] and observed, dipolar contacts among heme pocket residues and between those residues are illustrated schematically in Figure 1. However, even a cursory comparison of the ^{1}H NMR spectra in Figure 2 reveals that the positions of the signals for the strongest dipolar-shifted residues, H_{CD1} of Phe43(CD1) and H_{FG5}, M_{FG5} of Ile99(FG5), are very similar for metMbCN complexes of **1**−**8**.

Heme Methyl ^{13}C Assignments. The ^{1}H-detected {^{1}H-^{13}C} HMQC spectrum of metMbCN containing native hemin **1** yielded the correlation for the four methyls (not shown) as reported earlier by heteronuclear COSY[51] and {H−^{13}C}-HMQC.[17] The {^{1}H−^{13}C}-HMQC spectrum of metMb(**2**)CN at 25 °C is displayed in Figure 3, in which the cross peaks in the ^{1}H dimension that correspond to the known six heme methyl ^{1}H shifts,[39] directly yield $\delta_{obs}(^{13}CH_3)$. These correlations were confirmed over the temperature range 15−35 °C. Similar spectra for metMbCN possessing hemins **3**−**8** (not shown) yield the $\delta_{obs}(^{13}CH_3)$ values for all complexes of interest, which are compared to the $^{13}CH_3$ shift for WT metMbCN in Table 1. The resulting δ_{hf} and $\delta_{con}(^{13}CH_3)$ are listed in Table 1 along with the published δ_{hf} proton data.[31,32,39−41]

Seating of the Hemin. Native protohemin, **1**, and its derivatives, hemins **2**, **7**, and **8**, (Figure 2) all have their propionates at the same positions, f(6) and g(7).[32,39,42] Hemin **3** has been shown[40] to orient with the lone propionate occupying either position f(6-) or g(7-), but only the former isomer, which is dominant, is considered here. Hemin **4** places its propionates

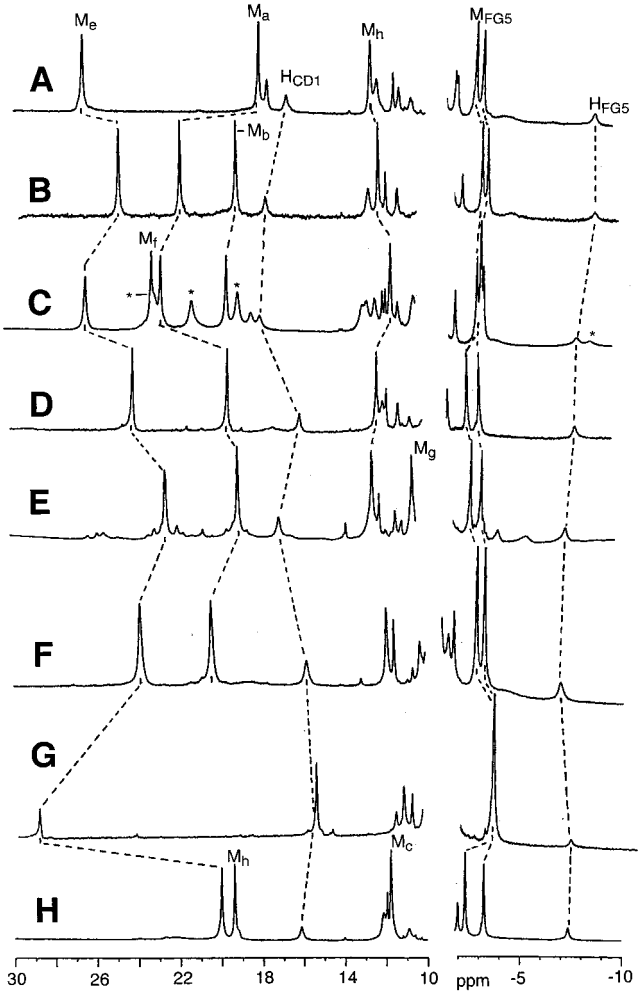

Figure 2. Resolved portions of the ^{1}H NMR spectra of the sperm whale metMb(***q***)CN complexes with variable hemin ***q*** in ^2H_2O, 50 mM phosphate, 100 mM NaCl at 25 °C, and pH 7.5−8.2 for (A) hemin **1** (native protohemin) at pH 7.6, (B) hemin **2** at pH 8.6, (C) hemin **3** at pH 8.0 (the asterisks show the location of the heme methyl peaks for the alternate hemin **3** orientation[40]), (D) hemin **4** at pH 7.5, (E) hemin **5** at pH 7.6, (F) hemin **6** at pH 8.0, (G) hemin **7** at pH 8.0, and (H) hemin **8** at pH 8.6. The heme methyl (M_i) and pyrrole $C_\alpha H$ (H_i) peaks are labeled by subscript i = a−h, that represents the position in the protein matrix as defined in Figure 1. The strongly dipolar-shifted Phe43(CD1) $C_\xi H$ (H_{CD1}) and Ile99(FG5) $C_\gamma H$ (H_{FG5}), $C_\delta H_3$ (M_{FG5}), and $C_\gamma H_3$ (M_{FG5}) peaks are labeled in (A), and the positions of these peaks in the other complexes are shown by dashed lines.

at positions b(2-) and f(6), while heme **5** has propionates at positions b(2-) and f(6-) (as well as at position g(7-)).[41] Etiohemin I (**6**) seats with methyls at positions a(1-), c(3-), e(5-), and g(7-).[43] The detailed orientation of a modified hemin about its normal relative to the protein matrix can be determined from the relative magnitudes of the steady-state NOEs from methyls at position a(M_a) and h(M_h) relative to the E helix backbone Val68(E11) $C_\alpha H$ and Ala71(E14) $C_\beta H_3$, or from methyls at positions c(M_c) and e(M_e) relative to Ile99(FG5) $C_\gamma H_3$ and $C_\delta H_3$, respectively.[28,30,43] These NOE patterns have been shown[40,41] to be essentially unchanged for hemins **2**, **6**, **7**, and **8** relative to WT (hemin **1**). Steady-state NOEs upon saturating these methyls in metMbCN reconstituted with hemin **3**−**5** reveal changes in relative NOEs of < 20% which translate to changes in orientation of < 3° about the heme normal[30,40,41] (not shown). Thus, it is reasonable to define the coordinates of methyls M_a−M_h as those that a methyl would have at positions 1−8 in the crystal structure of MbCO.[50]

(50) Kuriyan, J.; Wilz, S.; Karplus, M.; Petsko, G. A. *J. Mol. Biol.* **1986**, *192*, 133−154.
(51) Yamamoto, Y. *FEBS Lett.* **1987**, *222*, 115−119.

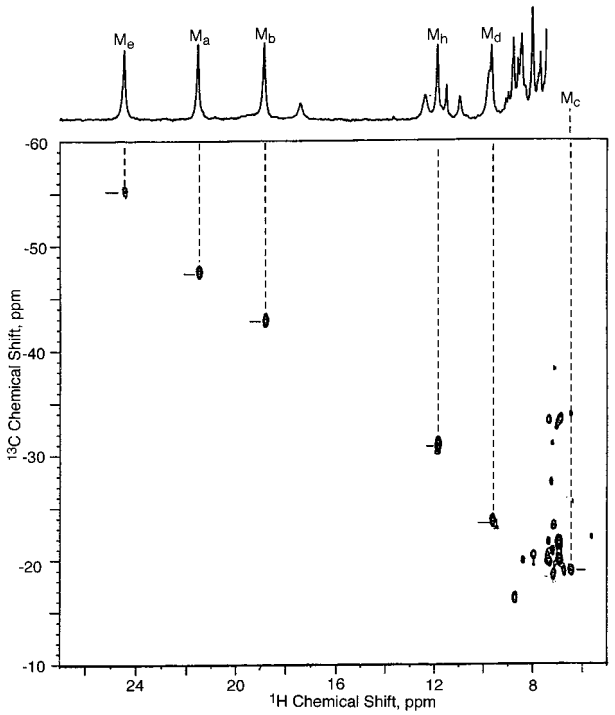

Figure 3. Portion of the ^{1}H detected {^{1}H−^{13}C}HMQC spectrum for the metMb(**2**)CN complex of hemin **2** (2,4-dimethyldeuteriohemin) in $^{2}H_2O$, 50 mM phosphate, and 100 mM NaCl at pH 8.0 at 25 °C. The known C^1H_3 assignments[39,41] lead to the $^{13}CH_3$ assignments as labeled M_a−M_e, and M_h showing the scalar ^{1}H−^{13}C cross peaks corresponding to the six assigned C^1H_3 peaks.

Magnetic Axes Determination. The resonances necessary to define the magnetic axes for the previously characterized metMbCN complexes of hemins **2** and **6**−**8** have been shown[32] to be very similar to those in WT,[31] and the reported magnetic axes are inconsequentially altered from those of WT (not shown; see Supporting Information). The assignments of the key heme pocket residues needed to define the magnetic axes were obtained for metMbCN reconstituted with hemin **3**−**5** on the basis of standard TOCSY and NOESY spectra (not shown), as described in detail earlier for metMbCN WT,[16] point mutants,[28,30] and complexes reconstituted with modified hemins.[32,43] The shifts are again very similar to those of the other complexes of hemins **1**, **2**, and **6**−**8**. The resulting chemical shifts are listed in Supporting Information. The magnetic axes for the eight complexes are all very similar (not shown) and can be described by a single orientation, $\alpha = 130 \pm 15°$, $\beta = 14 \pm 2°$, and $\kappa = -10 \pm 15°$, where the uncertainties include both the range of values obtained for different complexes and the intrinsic uncertainties for any single determination.[31] Hence, the dipolar shifts for all complexes, and the uncertainties, are obtained from the set of magnetic axes, with calculated $\delta_{dip}(^{13}CH_3)$ and $\delta_{dip}(C^1H_3)$ included in Table 1. The uncertainties in δ_{dip}(calc) are determined by the range of values calculated for the uncertainties in α, β, γ. By far, the largest uncertainty is due to the contribution from the rhombic anisotropy, which, when opposite in sign to the contribution from the axial term, leads to uncertainties in δ_{dip} as large as 40% (the largest for positions b and f). The resulting δ_{con} exhibit the uncertainties of both δ_{dia} and δ_{dip} and are listed in Table 1.

Discussion

Active Site Molecular Structure. The observation of very similar chemical shifts for noncoordinated amino acid residues, the same paramagnetic relaxation (all Phe43(CD1) $T_1(C_\zeta H) \sim 20$ ms, and all Ile99(FG5) $T_1(C_\gamma H) \sim 65$ ms), and the same NOESY contacts among these residues and to the heme, (see Figure 1) as observed in WT metMbCN,[42] attest to the strongly conserved structure in both the proximal and distal sides of the heme, as discussed previously[32,42,43] for the complexes of **1**, **2**, **7**, and **8**. The structural conservation is emphasized by the very similar magnetic axes and axial His F8 ring CH hyperfine shifts among all eight complexes.[52] The tilt of the major axes is $14 \pm 2°$ in a direction given by $\alpha \sim 130 \pm 15$ and has been proposed[16,28] to reflect the tilt of the Fe−CN vector toward pyrrole C by interacting with both His64(E7) and Val68(E11).

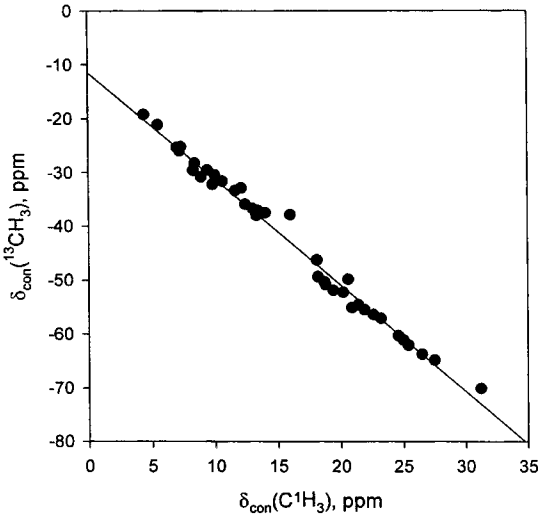

Figure 4. Plot of $\delta_{con}(C^1H_3)$ vs $\delta_{con}(^{13}CH_3)$ for all heme methyls of the metMb(***q***)CN complexes of hemins **1**−**8**. The straight line is the best fit to the data points and yields an intercept of −10 ppm for $\delta_{con}(^{13}CH_3)$ when $\delta_{con}(C^1H_3)$ is zero.

Origin of the Contact Shifts. It is noted that the form of δ^{L}_{dip} for a heme methyl ^{13}C is such that it is proportional[14,53,54] to the delocalized π spin density at the adjacent pyrrole carbon, ρ_π, that is,

$$\delta^{L}_{dip}(^{13}CH_3) = \epsilon\delta_{con}(^{13}CH_3) \qquad (6)$$

so that

$$\delta_{con}(^{13}CH_3) = [\delta_{hf}(^{13}CH_3) - \delta^{M}_{dip}(^{13}CH_3)][1 + \epsilon]^{-1} \qquad (7)$$

where ϵ is a (small) proportionality constant. Hence, a plot of δ_{con} ($^{13}CH_3$) versus δ_{con} (C^1H_3) should yield a straight line with an intercept of zero[54,55] (whether or not $\epsilon = 0$). Such a plot for all methyls in the metMbCN complexes of hemins **1**−**8** is shown in Figure 4. The data points fall on a straight line whose calculated intercept is −10 ppm and not zero, although the intercept is zero within experimental uncertainty. The expectation that the data should fall strictly on a straight line through the origin was the basis for an earlier innovative

(52) The $C_\epsilon H$ ring proton δ_{hf} of His F8 is dominated by δ_{dip} and has been shown to be exquisitely sensitive to changes in magnetic axes among metMbCN mutants.[31] The essentially unaltered shifts for both the $C_\epsilon H$ (19.3 ± 0.5 ppm) and $C_\delta H$ (−4.2 ± 0.5 ppm) (see Supporting Information) among the complexes of hemin **1**−**8** strongly support highly conserved magnetic axes.

(53) Yamamoto, Y.; Nanai, N.; Chujo, R.; Suzuki, T. *FEBS Lett.* **1990**, *264*, 113−116.

(54) Yamamoto, Y.; Nanai, N.; Chujo, R. *J. Chem. Soc., Chem. Commun.* **1990**, 1556−1557.

(55) Yamamoto, Y.; Komori, K.; Nanai, N.; Chujo, R.; Inoue, Y. *J. Chem. Soc., Dalton Trans.* **1992**, 1813−1819.

approach to determining magnetic axes.[54,56] The predicted ratio of $\delta_{con}(^{13}CH_3)/\delta_{con}(C^1H_3)$ is in the neighborhood of ~ -2.2 based solely on π spin density on the pyrrole carbon[6] (eq 2). The observed ratio, $\delta_{con}(^{13}CH_3)/\delta_{con}(C^1H_3)$, (assuming that the ligand-centered dipolar shift, δ^L_{dip}, can be neglected) is essentially constant at -2.6 ± 0.3 and independent of spin density for all methyls except those with very small (<10 ppm) proton shifts (Table 1).[17] Hence, the data are consistent with a small and negligible $\delta^L_{con}(^{13}CH_3)$ in eq 3. It is likely that both the failure to obtain an intercept of zero in Figure 4 and the deviation of the $\delta_{con}(^{13}CH_3)/\delta_{con}(C^1H_3)$ ratio from -2.6 for small δ_{con} is due to problems in determining $\delta_{con}(C^1H_3)$ when ρ_π is small.

The spin density, ρ_π, determined from δ_{con} for proton shifts has inherently more uncertainty than that obtained from ^{13}C shifts. This is due to the fact that the large uncertainty in $\kappa \pm 10°$ and the rhombic axes derived from the magnetic axes determination, together with the $\sim 3°$ uncertainty in heme rotational position, translate into substantial (to 1.8 ppm) uncertainties in δ_{dip}. These uncertainties translate to a much smaller uncertainty in $\delta_{con}(^{13}CH_3)$ than $\delta_{con}(C^1H_3)$ because $\delta_{con}(^{13}CH_3)$ is much larger than $\delta_{dip}(^{13}CH_3)$, and $\delta_{hf}(^{13}CH_3)$ is numerically the *sum* of the contact and dipolar contribution. However, $\delta_{hf}(C^1H_3)$ is numerically the *difference* between the magnitudes of δ_{con} and δ_{dip}, and the two contributions are comparable. The more reliable role of $\delta_{hf}(^{13}CH_3)$ than $\delta_{hf}(C^1H_3)$ in reflecting axial His orientation has been recognized[18,21,22,38] for some time and rested primarily on the fact that δ_{con} dominates δ_{hf} only for ^{13}C. The present analysis establishes that ^{13}C data are more reliable than ^1H data even if the magnetic axes and molecular structure are available.

It is observed that the $^{13}C/^1H$ contact shift ratio starts to become numerically larger, for smaller ρ_π, particularly for 3-CH_3 (see Table 1), and a question arises as to whether this represents a distortion of the heme near 3-CH_3 or whether it results simply from the fact that ρ_π is small, and hence, $\delta_{con}(C^1H_3)$ is the most uncertain of the four heme methyls. The latter basis is supported by the data on metMb(**8**)CN in Table 1, where δ_{con} is large for 3-CH_3, but small for 1-CH_3, because of the perturbation of the strongly electron withdrawing acetyl group. Indeed, now 3-CH_3 exhibits a "normal" ratio of -2.7, and the ratio for 1-CH_3 rises to -3.3.

Effect of Heme Peripheral Protein Contacts on π Spin Density Asymmetry. Both the δ_{con} and δ^M_{dip} are expected to reflect inversion symmetry through the iron. For native protohemin, **1**, the presence of an asymmetric heme substituent destroys this inversion symmetry even outside the protein matrix.[35−37] A measure of the asymmetry can be found in the ratio of the more reliable heme methyl ^{13}C contact shifts,[57] $\delta(^{13}CH_3)^i/\delta(^{13}CH_3)^j$, for two methyls, *i*, *j*, related by (true or pseudo) inversion symmetry. These ratios for the different methyls for hemins **1**−**8** are listed in Table 2. The available ratios are large for hemins **1**, **7**, and **8**, because the strongly perturbing vinyl and acetyl substituents destroy the inversion symmetry even outside the protein matrix.[17,32,36,51] However, for the pseudoinversion-symmetric hemins **2**−**4** and the truly inversion-symmetric hemins **5** and **6**, *the ratio for three of the positions is not 1.0 but is larger and essentially the same among hemins* **2**−**6**. The inversion asymmetry appears significant and comparable for 5-CH_3/1-CH_3, 8-CH_3/4-CH_3, and 6-CH_3/2-CH_3 but is minimal for 7-CH_3/3-CH_3, as shown in Table 2.

Table 2. Inversion asymmetry in Hemin Methyl ^{13}C Contact Shifts as Reflected in Ratios for Pairs of Inversion-Related Methyls[a]

hemin	δ_{con}(5-$^{13}CH_3$)/ δ_{con}(1-$^{13}CH_3$)	δ_{con}(6-$^{13}CH_3$)/ δ_{con}(2-$^{13}CH_3$)	δ_{con}(7-$^{13}CH_3$)/ δ_{con}(3-$^{13}CH_3$)	δ_{con}(8-$^{13}CH_3$)/ δ_{con}(4-$^{13}CH_3$)
1	1.40 ± 0.04			
2	1.14 ± 0.02			1.21 ± 0.04
3	1.15 ± 0.02	1.12 ± 0.03		1.22 ± 0.04
4	1.18 ± 0.03			
5	1.14 ± 0.02		1.02 ± 0.02	1.15 ± 0.04
6	1.15 ± 0.02		1.00 ± 0.02	
7	1.85 ± 0.05			
8	1.96 ± 0.06			

[a] At 30 °C determined from data as given in Table 1.

Two important conclusions can be drawn from the data in Table 2. First, it is noted that the inversion symmetry in $\delta_{hf}(^{13}CH_3)$ is absent for all but one position (the 3-CH_3/7-CH_3 pair) even in the two hemins, **5** and **6**, *with true inversion symmetry, and hence heme−protein interaction other than through the axial His must contribute to the rhombic asymmetry*. Second, the degree of the asymmetry, as measured in the $\delta_{con}(^{13}CH_3)$ ratio for inversion-related methyls, is essentially the same in the truly (**5**, **6**), and pseudo- (**2**, **3**−**5**), inversion-symmetric hemins. The latter point argues against significant influences of heme deformation on ρ_π asymmetry, because the variable sizes of methyl, ethyl, and propionate groups should induce differential distortions in the heme skeleton for hemin **2**−**6**. Thus, it may be expected that hemin **2**, which is much more readily reconstituted into *b*-type hemoproteins[58] than hemins **3**−**6**, can serve as a reliable pseudoinversion-symmetric hemin to probe for protein-based rhombic influences in other such proteins.

The pattern of deviation from 1.0 of $\delta^i_{con}(^{13}CH_3)/\delta^j_{con}(^{13}CH_3)$ for inversion-related methyls *i* and *j* suggests a pseudo-2-fold axis for this rhombic perturbation that passes approximately through 1-CH_3 and 5-CH_3, as reflected in the ratios in Table 2. Essential inversion symmetry is observed solely for δ_{con}(3-$^{13}CH_3$) and δ_{con}(7-$^{13}CH_3$). Among the numerous residue−heme contacts in Mb, two stand out in providing aromatic rings stacked approximately parallel to the heme plane, that from the invariant Phe43(CD1) ring on the distal, and that from the His97(FG3) imidazole ring on the proximal side.[50] $\pi-\pi$ interactions with the heme for the rings of Phe CD1 and His FG3 have been implicated as modulators of reactivity in globins.[59,60] The asymmetry is significant and comparable for the methyl pairs 5-CH_3/1-CH_3, 8-CH_3/4-CH_3, and 6-CH_3/2-CH_3, which appear to correlate with the positions of the two aromatic rings. The center of the asymmetry is along the 5-CH_3/1-CH_3 line. The 3-CH_3 and 7-CH_3, whose vector lies perpendicular to the 1-CH_3/5-CH_3 vector, exhibit very close to inversion symmetry (Table 2). Hence, the protein-induced asymmetry in truly inversion-symmetric hemins, as well as pseudoinversion-symmetric hemins, can be correlated with the position of $\pi-\pi$ contacts between hemin and aromatic residues. While globin mutants missing the completely invariant Phe43(CD1) are too unstable to serve in testing this hypothesis, there are numerous globins which are missing the FG3 position aromatic ring.[61]

(56) Yamamoto, Y.; Iwafune, K.; Nanai, N.; Osawa, A.; Chujo, R.; Suzuki, T. *Eur. J. Biochem.* **1991**, *198*, 299−306.

(57) It is important to note that the uncertainties in $\delta_{con}(^{13}CH_3)$ for calculating the contact shift ratio for inversion-related methyls are much lower (about one-third) than those reported in Table 1, because the large contribution from the uncertain rhombic axes is not relevant, as the values are identical for inversion-related methyls.

(58) Lee, K.-B.; Jun, E.; La Mar, G. N.; Rezzano, I.; Pandey, R. K.; Smith, K. M.; Walker, F. A.; Buttlaire, D. H. *J. Am. Chem. Soc.* **1991**, *113*, 3576−3583.

(59) Rousseau, D. L.; Shelnutt, J. A.; Ondrias, M. R.; Friedman, J. M.; Henry, E. R.; Simon, S. R. In *Hemoglobin and Oxygen Binding*; Ho, C., Ed.; Elsevier/North-Holland: New York, 1982; pp 223−229.

(60) Krishnamoorthi, R.; La Mar, G. N. *Eur. J. Biochem.* **1984**, *138*, 135−140.

These π contact contributions to the asymmetry in the π spin density of the hemin will interfere with the quantitative deduction of the His orientation from the $\delta_{con}(^{13}CH_3)$ pattern in any cyanide ligated ferric globin or peroxidase. It is noteworthy that cytochromes generally do not possess aromatic rings π-stacked parallel to the heme, and at least in cytochrome *c*, where the heme should possess pseudo-inversion symmetry outside the protein matrix, the δ_{con} ($^{13}CH_3$) appears to more closely reflect inversion symmetry[38] than in globins. Ferricytochrome b_5 reconstituted with the pseudoinversion-symmetric hemin **2** has yielded ^{1}H NMR spectra[58] where the δ_{hf} for 1-CH_3 ($\sim$12 ppm) and 5-CH_3 ($\sim$18 ppm) argue for a role of heme−protein contacts other than those of the two axial His ligands in modulating its rhombic asymmetry. More extensive, both ^{1}H and ^{13}C NMR studies with other pseudosymmetric hemins are necessary before determining if the aromatic rings stacked perpendicular to the hemin[62] in ferricytochrome b_5 are responsible for this asymmetry.

Acknowledgment. This work was supported by National Institutes of Health Grants HL 16087 (G.N.L.) and HL 22252 (K.M.S.). The funds for purchase of the NMR instrument were provided by NSF Grant 9724412.

Supporting Information Available: One table (chemical shifts for heme pocket residues for metMb(**q**)CN with hemins **q = 1-6**); 2 pages (pdf). This material is available free of charge via the Internet at http://pubs.acs.org.

JA011175R

(61) Dayhoff, M. O. *Atlas of Protein Sequence and Structure*; National Biomedical Research Foundation: Washington, DC, 1972; Vol. 5.

(62) Mathews, F. S.; Argos, P.; Levine, M. *Cold Spring Harbor Symp. Quant. Biol.* **1971**, *36*, 387−395.